Dynamics of Astrophysical Discs

The proceedings of a conference
at the Department of Astronomy,
University of Manchester,
13 - 16 December 1988.

Edited by

J. A. SELLWOOD

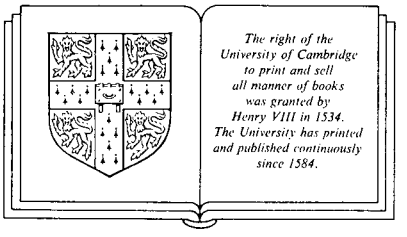

CAMBRIDGE UNIVERSITY PRESS

Cambridge

New York Port Chester

Melbourne Sydney

Published by the Press Syndicate of the University of Cambridge
The Pitt Building, Trumpington Street, Cambridge CB2 1RP
40 West 20th Street, New York, NY 10011, USA
10 Stamford Road, Oakleigh, Melbourne 3166, Australia

First published 1989

Printed in Great Britain at the University Press, Cambridge

British Library cataloguing in publication data available

Library of Congress cataloguing in publication data available

ISBN 0 521 37485 5

Table of contents

Titles of invited papers are **highlighted**. *Names of co-authors who did not attend the conference are given in smaller type.*

Spiral waves in Saturn's rings

Jack J. Lissauer*
State University of New York, Stony Brook, USA

Abstract Spiral density waves and spiral bending waves have been observed at dozens of locations within Saturn's rings. These waves are excited by resonant gravitational perturbations from moons orbiting outside the ring system. Modelling of spiral waves yields the best available estimates for the mass and the thickness of Saturn's ring system. Angular momentum transport due to spiral density waves may cause significant orbital evolution of Saturn's rings and inner moons. Similar angular momentum transfer may occur in other astrophysical systems such as protoplanetary discs, binary star systems with discs and spiral galaxies with satellites.

1 Introduction

Saturn's ring system was the first astrophysical disc to be discovered. When Galileo observed the rings in 1610, he believed them to be two giant moons in orbit about the planet. However, these "moons" appeared fixed in position, unlike the four satellites of Jupiter which he had previously observed. Moreover, Saturn's "moons" had disappeared completely by the time Galileo resumed his observations of the planet in 1612. Many explanations were put forth to explain Saturn's "strange appendages", which grew, shrank and disappeared every 15 years. In 1655, Huygens finally deduced the correct explanation, that Saturn's strange appendages are a flattened disc of material in Saturn's equatorial plane, which appear to vanish when the Earth passes through the plane of the disc (Figure 1). The length of time between Galileo's first observations of Saturn's rings and Huygens' correct explanation was due in part to the poor resolution of early telescopes. However, a greater difficulty was recognition of the possibility and plausibility of astrophysical disc systems. Contrast this to the situation today, when almost any flattened object observed in the heavens is initially suspected of being a disc.

The understanding of Saturn's ring system progressed slowly in the three centuries following Huygens [see Alexander (1962) for a historical review]. During this period, attention gradually shifted away from Saturn's rings as other astrophysical discs were observed (*e.g.* spiral galaxies) or proposed based on theoretical considerations (*e.g.* the protoplanetary disc, Kant 1745, Laplace 1796).

Similarities between Saturn's rings and spiral galaxies were first remarked upon by Maxwell (1859) "I am not aware that any practical use has been made of Saturn's Rings ... But when we contemplate the Rings from a purely scientific point of view, they become the most remarkable bodies in the heavens, except, perhaps, those still less useful bodies – the spiral nebulae". Today we know that the type of waves responsible for the grand design spiral structure observed in many disc galaxies (Lin & Shu 1964) are also present on much smaller scale within Saturn's rings (Cuzzi *et al.* 1981). The presence of density waves within Saturn's rings was predicted on theoretical grounds by Goldreich & Tremaine (1978a). Spiral bending waves, first proposed to explain galactic warps (Hunter & Toomre 1969), have also been observed within the rings of Saturn

* Alfred P. Sloan Research Fellow

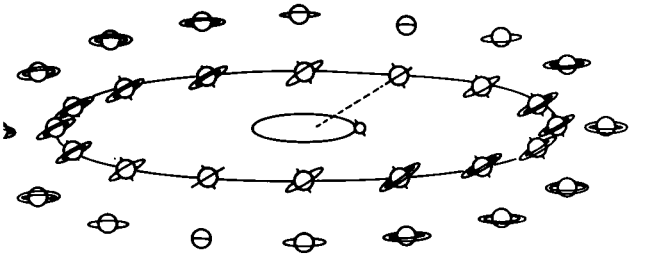

Figure 1. Schematic of Saturn and its rings as viewed from Earth at various longitudes of Saturn's orbit.

(Shu, Cuzzi & Lissauer 1983, henceforth SCL). Angular momentum transport by spiral density waves may be important to Saturn's rings, the proto-solar nebula, galaxies and other astrophysical accretion discs.

Knowledge of planetary rings increased manifold during the decade from 1977 to 1986. Within this period ring systems were discovered about Uranus (Elliot *et al.* 1977), Jupiter (Smith *et al.* 1979) and Neptune (Hubbard *et al.* 1986). Spacecraft visited all of the ringed planets except Neptune, including three flybys of Saturn. Theoretical developments advanced almost as rapidly as observations.

Each of the planetary ring systems has its own distinctive character. Good general reviews are available for each ring system (Jupiter: Burns *et al.* 1984; Saturn: Cuzzi *et al.* 1984; Uranus: Cuzzi & Esposito 1987; Neptune: Nicholson *et al.* 1989). This review will focus on spiral density waves and spiral bending waves in planetary rings. Spiral waves generated by gravitational perturbations of external moons have been observed at several dozen locations within Saturn's rings and have tentatively been detected within the rings of Uranus (Horn *et al.* 1988). They represent one of the best understood forms of structure within planetary rings, and have been very useful as diagnostics of ring properties such as surface mass density and local thickness. However, the angular momentum transfer associated with the excitation of density waves within Saturn's rings leads to characteristic orbital evolution time-scales of Saturn's A ring and inner moons which are much shorter than the age of the solar system.

The theory of spiral waves in Saturn's rings is reviewed briefly in §2. §3 discusses the observations and the ring properties derived therefrom. The short timescale of ring evolution predicted by density wave torques and other outstanding questions are discussed in §4. Conclusions are summarized in §5.

2 Theory

Spiral density waves are horizontal density oscillations which result from the bunching of streamlines of particles on eccentric orbits (Figure 2). Spiral bending waves, in contrast, are vertical corrugations of the ring plane resulting from the inclinations of

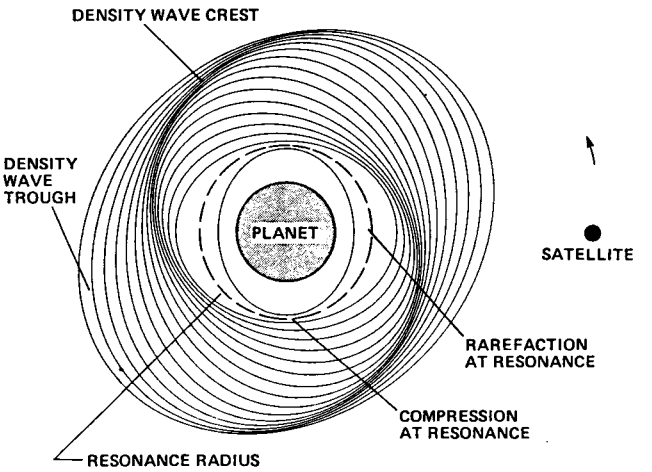

Figure 2. Schematic of particle streamlines within a resonantly excited two-armed spiral density wave. Density waves observed in Saturn's rings are much more tightly wound. (From Lissauer & Cuzzi 1985)

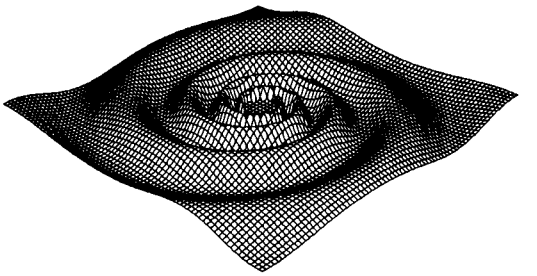

Figure 3. Schematic of a spiral bending wave showing variation of vertical displacement with angle and radius for a two-armed spiral. Bending waves observed in Saturn's rings are much more tightly wound. (From SCL)

particle orbits (Figure 3). In Saturn's rings, both types of spiral waves are excited at resonances with Saturn's moons, and propagate due to the collective self-gravity of the particles within the ring disc.

Ring particles move along paths which are very nearly Keplerian ellipses with one focus at the centre of Saturn. However, small perturbations due to the wave force a coherent relationship between particle eccentricities (in the case of density waves) or inclinations (in the case of bending waves) that produces the observed spiral pattern. The theory of excitation and propagation of linear spiral waves within planetary rings has been reviewed by Shu (1984). An abbreviated summary of aspects of the waves which may be observed and analyzed to determine ring properties is presented below.

2.1 ORBITS AND RESONANCES

Saturn's oblateness produces a gravitational potential different from that of a point mass. Near Saturn's equatorial plane, at an arbitrary distance, r, from the centre of the planet, the vertical frequency of a test particle, $\mu(r)$, exceeds its angular frequency, $\Omega(r)$, which in turn exceeds the radial (epicyclic) frequency, $\kappa(r)$. Thus the nodes of a particle's orbit regress and the line of apsides advances (*e.g.* Burns 1976).

Resonances occur where the epicyclic (or vertical) frequency of the ring particles is equal to the frequency of a component of a satellite's horizontal (vertical) forcing, as sensed in the rotating frame of the particle. We can view the situation as the resonating particle always being at the same phase in its radial (vertical) oscillation when it experiences a particular phase of the satellite's forcing. This situation enables continued coherent "kicks" from the satellite to build up the particle's radial (vertical) motion, and significant forced oscillations may thus result.

The locations and strengths of resonances with any given moon can be determined by decomposing the gravitational potential of the moon into Fourier components [see Shu (1984) for details]. The disturbance frequency, ω, can be written as the sum of integer multiples of the satellite's angular, vertical and radial frequencies:

$$\omega = m\Omega_{\rm M} + n\mu_{\rm M} + p\kappa_{\rm M}, \tag{1}$$

where the azimuthal symmetry number, m, is a non-negative integer, and n and p are integers, with n being even for horizontal forcing and odd for vertical forcing. The subscript M refers to the moon. Horizontal forcing, which can excite density waves and open gaps by angular momentum transport, occurs at inner Lindblad resonances, $r_{\rm L}$, where

$$\kappa(r_{\rm L}) = m\Omega(r_{\rm L}) - \omega. \tag{2}$$

Vertical forcing occurs at inner vertical resonances, $r_{\rm V}$, where

$$\mu(r_{\rm V}) = m\Omega(r_{\rm V}) - \omega. \tag{3}$$

When $m \neq 1$, the approximation $\mu \approx \Omega \approx \kappa$ may be used to obtain

$$\frac{\Omega(r_{\rm L,V})}{\Omega_{\rm M}} = \frac{m+n+p}{m-1}. \tag{4}$$

The $(m+n+p)/(m-1)$ or $(m+n+p) : (m-1)$ notation is commonly used to identify a given resonance.

Lindblad resonances with $m = 1$ depend on apsidal precession due to the difference between $\Omega(r)$ and $\kappa(r)$ and are referred to as apsidal resonances. Vertical resonances with $m = 1$ depend on the regression of the nodes of the ring particles upon the ring plane caused by the difference between $\Omega(r)$ and $\mu(r)$ and are called nodal resonances.

The strength of the forcing by the satellite depends, to lowest order, on the satellite's eccentricity, e, and inclination, i, as $e^{|p|}(\sin i)^{|n|}$. The strongest horizontal resonances have $n = p = 0$, and are of the form $m : (m-1)$. The strongest vertical resonances have $n = 1$, $p = 0$, and are of the form $(m+1) : (m-1)$. The locations and strengths of such orbital resonances are easily calculated from known satellite masses and orbital

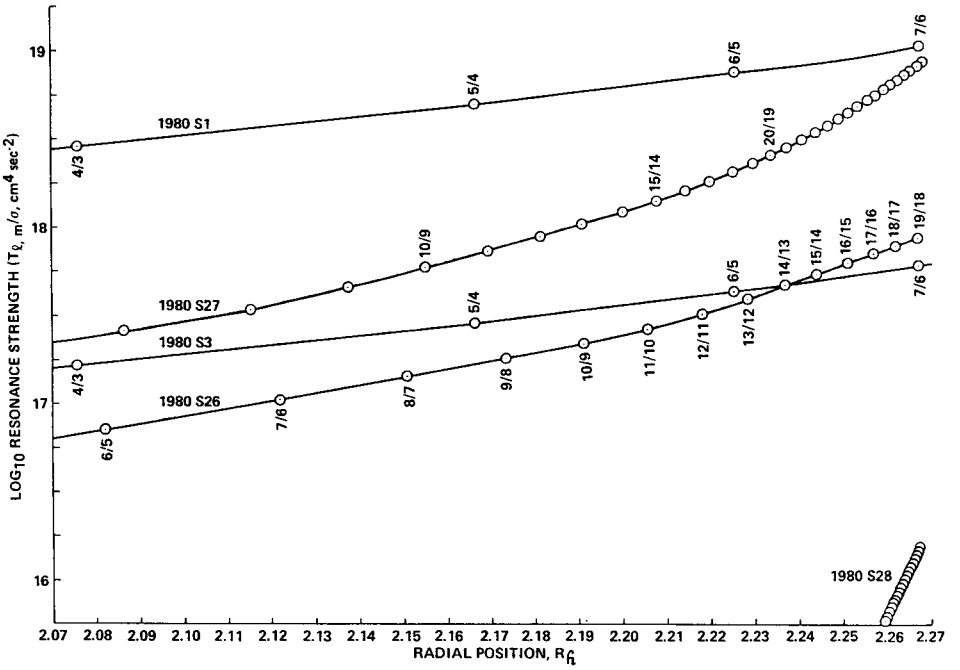

Figure 4. Locations and strengths of major Lindblad resonances in Saturn's A ring for Saturn's five closest "ring moons", Janus (1980S1), Epimetheus (1980S3), Pandora (1980S26), Prometheus (1980S27) and Atlas (1980S28). The closer moons have more closely spaced resonances with strength increasing outward more rapidly. (From Lissauer & Cuzzi 1982)

parameters and the gravitational moments of Saturn (Lissauer & Cuzzi 1982, SCL). By far the lion's share of the strong resonances lie within the outer A Ring (Figure 4).

2.2 BENDING WAVES

The vertical component of the gravitational force exerted by a satellite on an orbit inclined with respect to the plane of the rings excites motion of the ring particles in a direction perpendicular to the ring plane. The vertical excursions of the particles are generally quite small (Burns *et al.* 1979). However, at vertical resonances in Saturn's rings, the natural vertical oscillation frequency of a particle, $\mu(r)$, is equal to the frequency at which the vertical force due to one Fourier component of the satellite's gravitational potential is applied. Such coherent vertical perturbations can produce significant out-of-plane motions (Cook 1976). Self-gravity of the ring disc supplies a restoring force that enables bending waves to propagate away from resonance creating a corrugated spiral pattern. For $m > 1$, bending waves propagate toward Saturn (SCL); nodal bending waves ($m = 1$) propagate away from the planet (Rosen & Lissauer 1988).

In the inviscid linear theory, where viscous damping is ignored and the slope of the bent ring mid-plane is assumed to be small, the height of the local ring mid-plane

relative to the Laplace (invariant) plane (Figure 5) is given by

$$Z(r) = \frac{|A_V|}{\sqrt{\pi}} \Re \left(e^{i(\Phi_V + \frac{\pi}{4})} e^{iq\xi^2} \int_{-\infty}^{\xi} e^{-iq\eta^2} d\eta \right) \tag{5}$$

where

$$|A_V| = \mathcal{F} \sqrt{\frac{r_V}{G\sigma|\mathcal{D}|}}, \tag{6}$$

$$\xi \equiv q(r_V - r) \sqrt{\frac{|\mathcal{D}|}{4\pi G\sigma r_V}}, \tag{7}$$

$$\mathcal{D} \equiv \left[r \frac{d}{dr} (\mu^2(r) - m^2 \big(\Omega_p - \Omega(r)\big)^2 \right]_{r=r_V}, \tag{8}$$

r is the distance from Saturn, r_V is the location of the vertical resonance and $\Omega_p = \omega/m$ is the angular frequency of the reference frame in which the wave pattern remains fixed (Gresh *et al.* 1986). The number of spiral arms in the wave is equal to the azimuthal symmetry number of the resonance, m. The surface mass density of the ring material is denoted by σ and G is the gravitational constant. The forcing strength, $\mathcal{F}$, and the phase of the wave, Φ_V, depend on the satellite in a manner given by equations (45-47) of SCL for $m > 1$ and equations (11-13) of Rosen & Lissauer (1988) for $m = 1$. The operator $\Re$ signifies the real part of the quantity. The sign of $\mathcal{D}$ is given by q, which is equal to +1 for inner vertical resonances, at which all observed bending waves are excited.

The oscillations of bending waves are governed by the Fresnel integral in equation (5). In the asymptotic far-field approximation, the oscillations remote from resonance have a wavelength

$$\lambda = \frac{4\pi^2 G\sigma}{m^2 [\Omega_p - \Omega(r)]^2 - \mu^2(r)}. \tag{9}$$

Equation (9) can be simplified by approximating the orbits of the ring particles as Keplerian, $\mu(r) = (GM_S/r^3)^{1/2} = \Omega(r)$, for the $m > 1$ case and approximating the departure from Keplerian behaviour to be due to the quadrupole term of Saturn's gravitational potential, $\frac{3}{2} J_2 \frac{R_S^2}{r^5} GM_S$, $J_2 = 0.0163$, for the $m = 1$ case. (The symbols M_S and R_S refer to the mass and equatorial radius of Saturn, respectively.) The resulting formulae are (Rosen 1989)

$$\lambda(r) \simeq 3.08 \left(\frac{r_V}{R_S} \right)^4 \frac{\sigma}{m-1} \frac{1}{r_V - r} \qquad (m > 1) \tag{10a}$$

$$\lambda(r) \simeq 54.1 \left(\frac{r_V}{R_S} \right)^6 \sigma \frac{1}{r_V - r} \qquad (m = 1) \tag{10b}$$

where λ, r and r_V are measured in kilometers, and σ is in g cm^{-2} . Equations (10) afford a means of deducing the surface density from measured wavelengths.

Inelastic collisions between ring particles act to damp bending waves. A rigorous kinetic theory of the damping of bending waves has not yet been developed. SCL used

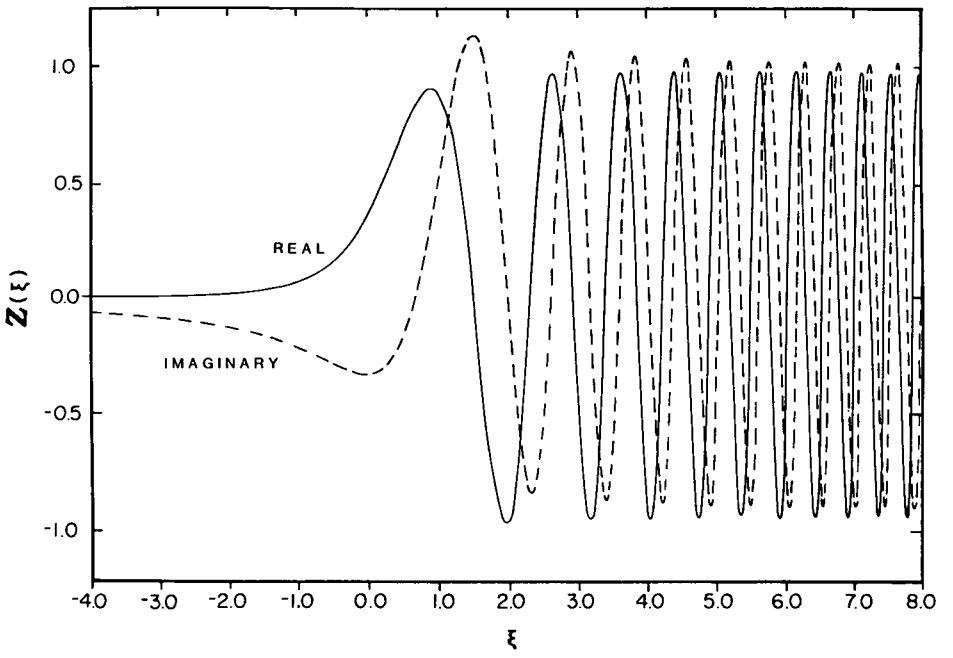

Figure 5. Theoretical height profile of an undamped linear spiral bending wave as a function of distance from resonance. The length and height scales are in arbitrary units. The solid and dashed lines represent two profiles of the same wave plotted at different azimuths. (Adapted from SCL)

a fluid approximation and the assumption that damping is weak to derive an amplitude variation of in terms of the viscosity of the ring material, ν. The collisional model of Goldreich & Tremaine (1978a) can be used to calculate the local scale height, H, of the ring from the measured viscosity:

$$H = \sqrt{\frac{2\nu}{\Omega}\frac{(1+\tau^2)}{\tau}} \tag{11}$$

where τ is the optical depth of the ring.

2.3 DENSITY WAVES

The gravity of a moon on an arbitrary orbit about Saturn has a component which produces epicyclic (radial and azimuthal) motions of ring particles. However, as in the case of vertical excursions induced by moons on inclined orbits, the epicyclic excursions are generally extremely small. An exception occurs near Lindblad (horizontal) resonances (equation 2), where coherent perturbations are able to excite significant epicyclic motions. In a manner analogous to the situation at vertical resonances, self-gravity of the ring disc supplies a restoring force that enables density waves to propagate away from Lindblad resonance (Goldreich & Tremaine 1978a). All density waves identified within

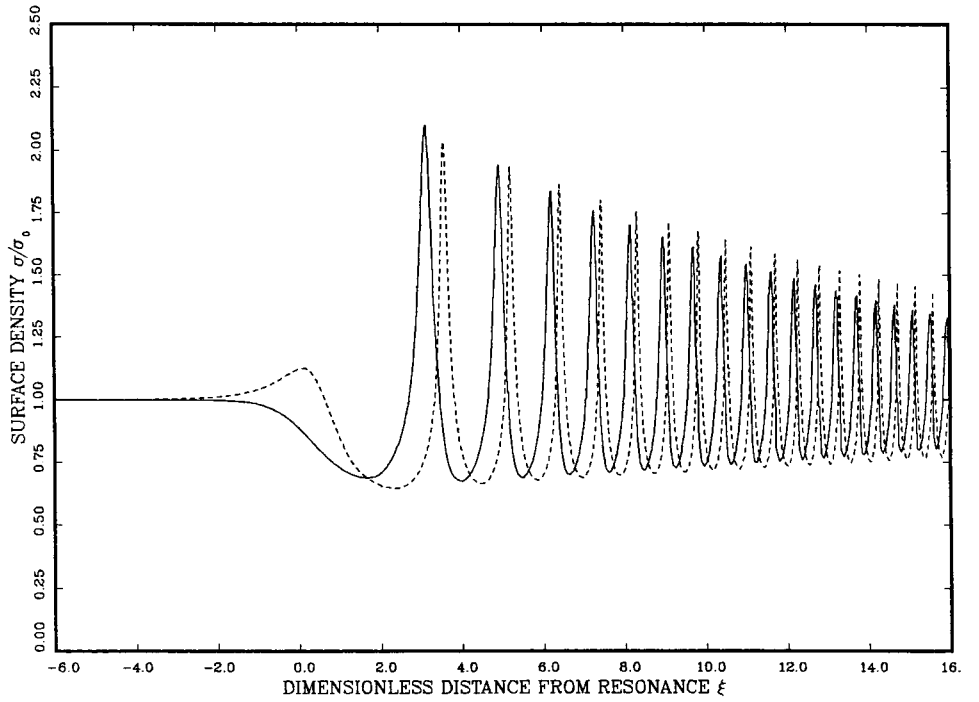

Figure 6. Theoretical surface density profile of a damped non-linear spiral density wave. The solid and dashed lines represent two profiles of the same wave plotted at different azimuths. (Adapted from Shu *et al.* 1985b)

Saturn's rings are excited at Inner Lindblad Resonances, and propagate outward, away from the planet.

The theory of spiral density waves is analogous to that of spiral bending waves, with the fractional perturbation in surface mass density, $\Delta\sigma/\sigma$, replacing the slope of the disc, dZ/dr. The relationship in the linear theory ($\Delta\sigma/\sigma \ll 1$) which is analogous to equation (5) is (Rosen 1989)

$$\frac{\Delta\sigma}{\sigma} = \Re\left\{A_{\rm L}\left[i + \xi_0 e^{-i\xi_0^2/2}\int_{-\infty}^{\xi_0} e^{i\eta^2/2}d\eta\right] e^{-im\theta_0}\right\} \tag{12}$$

where i denotes $\sqrt{-1}$ and the amplitude is given by

$$A_{\rm L} = \frac{-\psi_{\rm M}}{2\pi G r_{\rm L}} \tag{13}$$

The forcing function, $\psi_{\rm M}$, is given for various cases by Shu (1984) and Rosen (1989). The phase of the wave is given by

$$\Phi_{\rm L} = \arg(A_{\rm L}) + \frac{\pi}{2} - m\theta_0 \tag{14}$$

Far from resonance, equation (12) predicts a spacing between wave crests given by

$$\lambda = \frac{4\pi G\sigma}{m^2[\Omega_p - \Omega(r)]^2 - \kappa^2(r)} \tag{15}$$

Equations (10), with R_V and r_V replaced by R_L and r_L, are valid for density waves under the same approximations as for bending waves. The theory of damping of linear density waves is given by Goldreich & Tremaine (1978a).

Most density waves observed in Saturn's rings have $\Delta\sigma/\sigma \sim 1$. At such large amplitudes the linear theory breaks down. The theory of non-linear density waves has been developed by Shu *et al.* (1985a, b) and Borderies *et al.* (1986). The principal results of the non-linear theory are as follows: non-linear density waves depart from the smooth sinusoidal pattern predicted by equation (12), and become highly peaked (Figure 6). The theoretical wave profiles have broad, shallow troughs with surface density never dropping below half of the ambient value, and are qualitatively similar to observed waves (compare Figures 6 and 10). (A more detailed correspondence may be achieved if the background surface density is assumed to vary within the wave region, Longaretti & Borderies 1986.) Shocks do not occur, *i.e.* neighbouring streamlines never cross, even though they become arbitrarily close at wave crests as the wave propagates outward if viscous damping is not included (Shu *et al.* 1985a). The non-linear torques exerted by Saturn's moons are similar to those calculated using linear theory (Shu *et al.* 1985b).

3 Observations

Spiral waves in planetary rings are extremely tightly wound, with typical winding angles being 10^{-4} to 10^{-3} degrees. Such waves have very short wavelengths, of order 10 km. Earth-based photographs and Pioneer spacecraft images have resolution inadequate to detect such small scale features, so all available observations of spiral waves in planetary rings are from the Voyager spacecraft. Stellar occultations by Saturn's rings visible from Earth and HST may provide additional data during the next few years.

Spiral waves in Saturn's rings were detected by four instruments on the Voyager spacecraft. Voyager images have been used to detect density waves due to brightness contrasts between crests and troughs both in reflected light on the sunlit face of the rings (Figure 7; Dones 1987) and in diffuse transmission of sunlight to the dark side of the ring plane (Cuzzi *et al.* 1981). Bending waves are visible on Voyager images of the lit face of the rings (Figure 7) due to the dependence of brightness on local solar elevation angle (SCL). Bending waves appear on images of the unlit face of the rings due to the dependence of the slant optical depth, through which sunlight diffused, on local ring slope (Lissauer 1985).

Both density waves and bending waves were detected in the data received when the Voyager radio signal was attenuated by the occulting rings on its way to Earth (Figure 8; Marouf *et al.* 1986, Gresh *et al.* 1986). Density waves are observable by occultation experiments because bunching of particle streamlines increases the optical depth, τ, of crests; bending waves, although they leave optical depth normal to the ring plane unchanged, can be detected because the tilt of the ring plane causes oscillations in the observed slant optical depth (Figure 9). Similarly, the Voyager Photopolarimeter

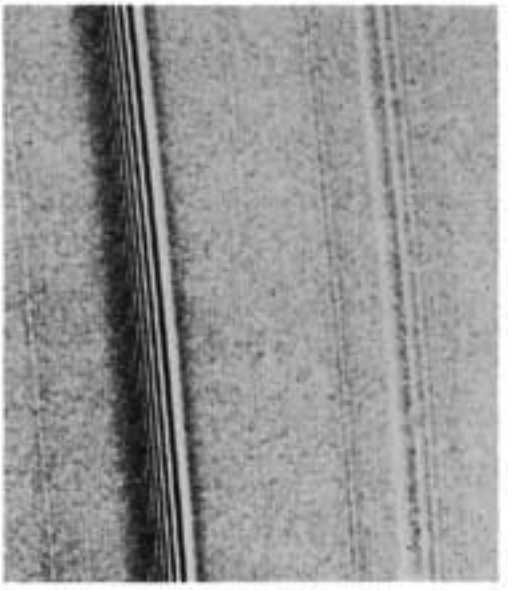

Figure 7. Voyager 2 image (FDS 43999.19) of a portion of the lit face of Saturn's A ring showing two prominent wave patterns. The feature on the left is the Mimas 5:3 bending wave; its contrast is high because the tilt of the local ring plane due to the wave was comparable to the solar elevation angle ($\sim 8°$) when the image was taken. The Mimas 5:3 density wave is seen on the right. The separation between the locations of the two waves is due to the non-closure of orbits caused by Saturn's oblateness. The other linear features in the images are unresolved density waves excited by the moons Pandora and Prometheus. Saturn is off to the left.

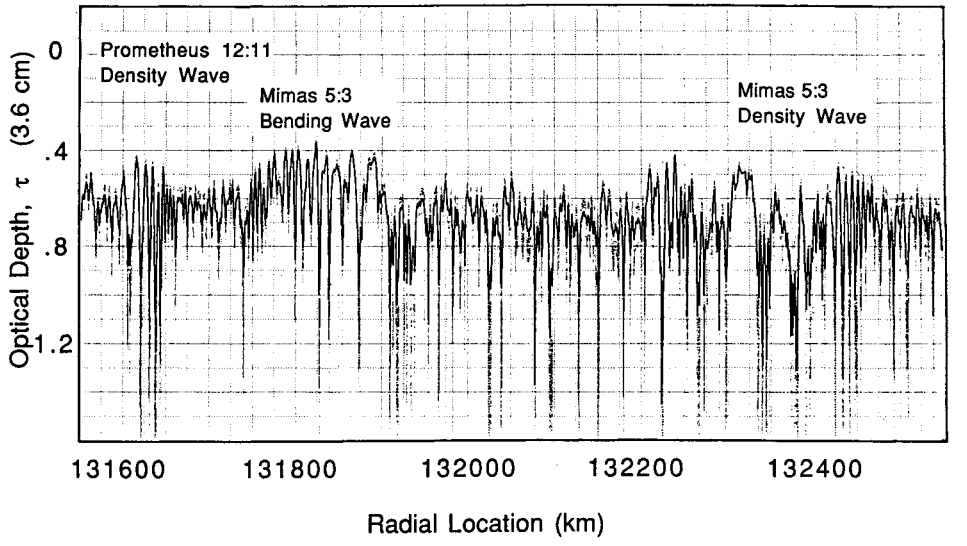

Figure 8. Examples of wave features observed in the radio occultation data of Saturn's A ring. The solid curved is measured normal optical depth, τ, plotted to increase downward. The gray shaded region represents the 70% confidence bounds on the measurement. (From Rosen 1989)

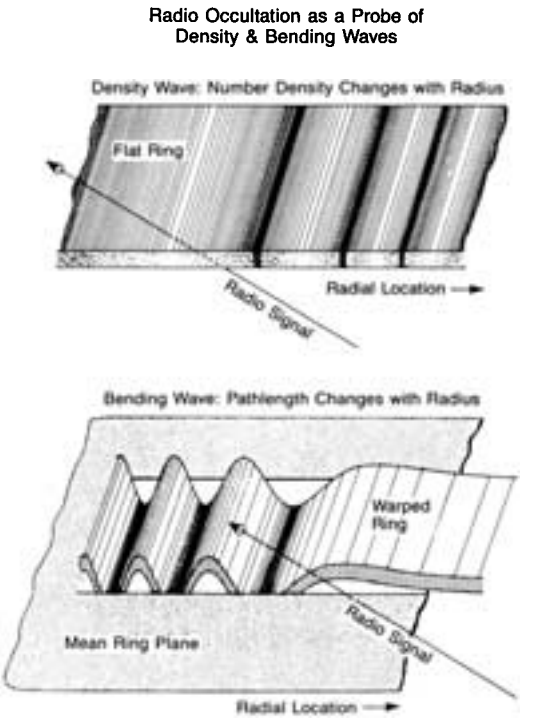

Figure 9. Schematic of a radio occultation of spiral waves. (From Rosen 1989)

(PPS) and Ultraviolet Spectrometer observed the diminution of light as a star passed behind the rings, thereby detecting changes in the slant optical depth of the rings caused by spiral waves (Lane *et al.* 1982, Holberg *et al.* 1982; Figure 10).

Five bending waves and several dozen density waves in Saturn's rings have thus far been identified with exciting resonances and analyzed to determine the local surface mass density of the rings. Results of the first analyses are tabulated by Esposito *et al.* (1984). More recent studies have been performed by Cuzzi *et al.* (1984), Lissauer (1985), Gresh *et al.* (1986), Longaretti & Borderies (1986), Rosen & Lissauer (1988) and Rosen (1989). The surface density, σ, at most wave locations in the optically thick A and B rings is of order 50 g cm^{-2}. Measured values in the optically thin C ring are $\sigma \approx 1$ g cm^{-2}; an intermediate value of 10 g cm^{-2} has been estimated for Cassini's Division.

The damping behaviour of three bending waves have also been analyzed to place upper bounds on the viscosity and local thickness of the rings (Lissauer *et al.* 1984, Esposito *et al.* 1983, Gresh *et al.* 1986, Rosen & Lissauer 1988). The A ring appears to have a local thickness of a few tens of meters; the thickness of the C ring is < 5 m. Viscosity measurements from the damping of density waves are less reliable (Lissauer *et al.* 1984, Shu *et al.* 1985b).

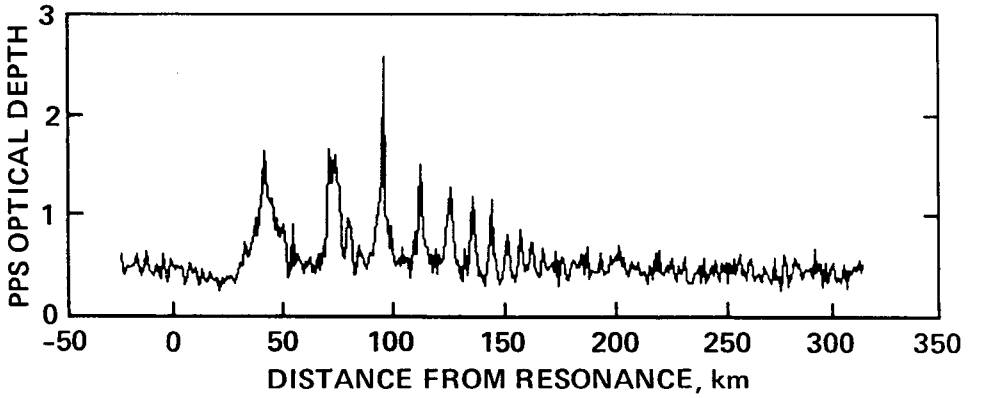

Figure 10. The Mimas 5:3 density wave as viewed from the Voyager 2 PPS stellar occultation experiment, plotted so that τ increases upwards. Note the sharp peaks and broad flat troughs caused by non-linearities (*cf.* Figure 6). (From Cuzzi *et al.* 1984)

The outer edges of the B and A rings are maintained by the Mimas 2:1 and Janus 7:6 resonances, which are the strongest resonances within the ring system (Smith *et al.* 1981, Holberg *et al.* 1982, Porco *et al.* 1984a, Lissauer & Cuzzi 1982, Borderies *et al.* 1982). Nearly empty gaps with embedded optically thick ringlets have been observed at strong resonances located in optically thin regions of the rings (Holberg *et al.* 1982). These features are probably caused by a resonance-related process; however, no explanation for the embedded ringlets currently exists. Nearly empty gaps with embedded ringlets have also been observed at non-resonant locations (Porco *et al.* 1984b).

4 Unresolved issues

Although spiral waves in Saturn's rings are well understood by astrophysical standards, there remain several major outstanding issues. These problems will be summarized in this section in a sequence beginning with those of an observational nature and ending with theoretical questions concerning angular momentum transport and the age of Saturn's rings. The latter issues are probably more relevant to the understanding of spiral waves in other disc systems.

The first mystery about density waves is why they are seen at all in Voyager images (Dones 1987). The optical depths of the A and B rings are sufficiently large and the solar elevation angles at the Voyager 1 and 2 encounters so low (4° and 8°, respectively) that very little sunlight could diffuse through the rings. This means that the brightness of the lit face of the rings should not be very sensitive to ring optical depth, as very little light would be able to diffuse down to the "extra" material near the unlit face, be reflected, and then diffuse back out to reach the Voyager cameras. The brightness contrast predicted by the wave amplitudes directly observed via stellar and radio occultations (which are generally similar to the theoretical amplitudes) is far less than the contrast observed in the images. All density waves imaged on the lit face of the rings are non-linear. The strong particle perturbations in such regions cause high-velocity collisions that can produce a physical thickening of the rings at density wave crests. The "top surface" of the ring plane could therefore vary in elevation, and local slopes could